Resonant optical nonlinearity of conjugated polymers

Ming-Che Chang*
Department of Physics, National Tsing Hua University, Hsinchu 300, Taiwan

Hsin-Fei Meng†
Institute of Physics, National Chiao Tung University, Hsinchu 300, Taiwan
(Received 13 December 1996; revised manuscript received 3 July 1997)

When the energy of a pump wave is in resonance with the exciton creation energy, the electric susceptibility of a conjugated polymer in response to the probe wave is altered by the exciton gas. In this paper we calculate the dependence of this change on the exciton populations by the equation of motion (EOM) method. The magnitude of optical nonlinearity is also influenced by ambient temperature, by the extent of exciton wave functions, and by the strength of electron-electron interaction. All of these factors can be easily incorporated in the EOM approach systematically. Using the material parameters for polydiacetylene, the optical Kerr coefficient n_2 obtained is about 10^{-8} cm^2/W, which is close to experimental value, and is four orders of magnitude larger than the value in nonresonant pump experiments. [S0163-1829(97)02743-4]

I. INTRODUCTION

As a class of materials promising for applications in all-optical devices for communication and data processing, conjugated polymers have been a subject of great research interest.[1] A conjugated polymer such as polydiacetylene (PDA) has long been recognized to exhibit large nonresonant third-order optical nonlinearities.[2] Most of the theoretical works on the nonlinear optics of these materials are based on the perturbative sum-over-state formula[3] that suits a *nonresonant* pumping well (but is inappropriate for resonant pumping). A fair agreement between experiments and theories has been achieved for a variety of nonresonant spectra, including two-photon absorption, third-harmonic generation, and electroabsorption.[4] In addition, the equation of motion (EOM) approach has also been employed in these studies.[5] The EOM for polarization, which is similar to the semiconductor Bloch equation originally used for inorganic semiconductors,[6] is a general tool whose validity goes beyond the perturbative regime[7] and will be used in this paper.

For conjugated polymers under *resonant* pumping, most of the optically excited electrons and holes remain bound at room temperature and form an exciton gas, instead of a plasma as in the III-V semiconductors.[8] This is because the magnitude of the exciton binding energy in conjugated polymers (of the order of 1 eV) is much larger than that in inorganic semiconductors (a few meV). This presents a difficult situation for the calculation of resonant nonlinearity. Even though there are numerous experimental works, few theoretical works have been devoted to this subject. A simple and heuristic explanation of this nonlinearity based on phase-space filling (PSF) has been proposed, and the result agrees quantitatively with experiments.[9] The esssence of PSF is that when there is a finite concentration of excitons, the phase space for further excitons to form is reduced because of the exclusion principle, and henceforth the probe absorption signal is reduced. The limitation of PSF is that it cannot predict the whole spectral response of the electric susceptibility, nor the effects of temperature, strength of electron-electron interaction, etc.

Motivated by the desire to have a more accurate theoretical tool to understand this phenomenon, we present a detailed analysis of the nonlinear susceptibility based on EOM. We will utilize the technique developed by Haug, Koch, and Schmitt-Rink to make a connection between exciton populations and the electron populations that appear in the EOM.[10] However, since the link is suitable for dilute exciton gas only, we shall concentrate our study in this regime. Furthermore, from the comparison between the lineshapes of time-resolved and cw photoluminescence spectra, the typical intraband scattering time is estimated to be less than a picosecond in polymers.[11] Therefore, it is possible to consider a simpler situation in which the exciton gas is in quasithermal equilibrium, and in which the population is determined by the intensity of the pump wave. Because of these approximations, phenomena such as exciton-exciton interaction, excited-state absorption, and off-equilibrium momentum distribution are not considered.

In this paper we have done extensive studies on the optical nonlinearity of PDA. There are several advantages in choosing this material: First, it has the largest nonresonant third-order nonlinearity of all polymers and very large resonant nonlinearity. Second, it is one of a few conjugated polymers that can form high-quality single crystals and is more amenable to theoretical analysis. Third, its chain-to-chain distance is large because of large side groups and, therefore, the interchain interaction is less important. Various aspects of the nonlinear spectra are investigated. By choosing a reasonable value of the Coulomb interaction strength, the resonant optical Kerr coefficient n_2 being calculated agrees very well with experiments. Furthermore, the effect of electron-electron interaction on the height and position of the exciton absorption peak is studied. We also study the influence of temperature, as well as the relative populations of singlet and triplet excitons, on the probe spectra. This work provides a systematic analysis of the influence of various microscopic parameters on the optical nonlinearity and may serve as a guide for the search for optical materials with larger resonant nonlinearities.

This paper is organized as follows. In Sec. II, the equation

 © 1997 The American Physical Society

of motion for polarization in conjugated polymers is derived. In Sec. III, the Coulomb potential matrix elements and electron occupation numbers are calculated. The numerical results are presented in Sec. VI, and Sec. V is the conclusion.

II. EQUATION OF MOTION FOR POLARIZATION

A conjugated polymer is a macromolecule with many electronic and ionic degrees of freedom. There have been several attempts to include both types of degrees of freedom in calculations on the electronic and optical properties of conjugated polymers. This is a very difficult task. To date, an exact solution for chains longer than 20 sites is still lacking.[12] It is especially challenging to calculate *resonant* optical nonlinearity by including the effects of electrons (including excitons) and phonons simultaneously. In this paper, we choose a modest approach and focus only on the electronic contribution to the nonlinearity. By doing so, we will not, for example, be able to produce satellite phonon peaks next to the main resonant absorption peak.[13] Our main goal is to calculate the optical nonlinearity due to the exciton gas, which is derived from the dependence of the magnitude of the main absorption peak on the exciton populations. In fact, Greene and co-workers[7,9] have demonstrated that the PSF model, whose origin is purely electronic, can explain major features of the spectra well. Furthermore, we consider only the dynamics of π electrons; the σ electrons are tightly bound to the ions and have little influence on the dynamical response. However, they do contribute to the renormalization of the interaction between π electrons, and between ions and π electrons. These effects appear implicitly through the parameters in the π-electron Hamiltonian.

Our calculation is based on the Su-Schrieffer-Heeger-like Hamiltonian with electron-electron interactions, $H=H_0+H_1+H_2$, where

$$H_0=\sum_{k\sigma}\left(\epsilon_{ck}a^{\dagger}_{ck\sigma}a_{ck\sigma}+\epsilon_{vk}a^{\dagger}_{vk\sigma}a_{vk\sigma}\right), \tag{2.1}$$

$$H_1=\sum_{\lambda_1\lambda_2\lambda_3\lambda_4}\sum_{k_1k_2k_3k_4}\mathcal{V}^{k_1k_2k_3k_4}_{\lambda_1\lambda_2\lambda_3\lambda_4}a^{\dagger}_{\lambda_1k_1\sigma}a^{\dagger}_{\lambda_2k_2\sigma'}a_{\lambda_3k_3\sigma'}a_{\lambda_4k_4\sigma}, \tag{2.2}$$

and

$$H_2=-E(t)\sum_{k\sigma}\left[\mu_{vc}(k)a^{\dagger}_{vk\sigma}a_{ck\sigma}+\mu_{cv}(k)a^{\dagger}_{ck\sigma}a_{vk\sigma}\right]. \tag{2.3}$$

In these equations, $\epsilon_{c,vk}$ are the energies for the dimerization-induced conduction and valence band, $\mathcal{V}^{k_1k_2k_3k_4}_{\lambda_1\lambda_2\lambda_3\lambda_4}$ are the Coulomb potential matrix elements ($\lambda=c,v$), and $\mu_{\lambda\lambda'}(k)$ are the dipole matrix elements. H_2 describes the coupling between polarization and the *probe* field $E(t)$ along the chain. The influence of the pump field will be accounted for when calculating the conduction electron populations in the next section. The potential matrix elements are

$$\mathcal{V}^{k_1k_2k_3k_4}_{\lambda_1\lambda_2\lambda_3\lambda_4}=\int d^3\mathbf{r}d^3\mathbf{r}'\Psi^{*}_{\lambda_1k_1}(\mathbf{r})\Psi^{*}_{\lambda_2k_2}(\mathbf{r}')\times V_{ee}(\mathbf{r}-\mathbf{r}')\Psi_{\lambda_3k_3}(\mathbf{r}')\Psi_{\lambda_4k_4}(\mathbf{r}), \tag{2.4}$$

where V_{ee} is the screened Coulomb interaction between the π electrons, and $\Psi_{\lambda k}$ are the Bloch states solved from H_0. The usual practice is to neglect, from the very beginning, the terms that do not conserve electron numbers in each band, which include half of the 16 terms that do not have equal numbers of c indices and v indices, plus $\mathcal{V}^{k_1k_2k_3k_4}_{vvcc}$ and $\mathcal{V}^{k_1k_2k_3k_4}_{cvcv}$.[14] This is reasonable in metals or inorganic semiconductors where the Coulomb interaction is weak, but is not necessarily valid in conjugated polymers where the Coulomb interaction is much stronger, as indicated by the large exciton binding energies. Therefore, these terms will be kept in the derivation until they are proven negligible. It will be shown later that the terms without equal numbers of c and v indices indeed make no contribution, but the $\mathcal{V}^{k_1k_2k_3k_4}_{vvcc}$ and $\mathcal{V}^{k_1k_2k_3k_4}_{cvcv}$ terms cannot be ignored. In fact, unlike all the other terms, these two terms do not conserve the electron and hole spin individually, thus are essential to the lifting of the fourfold degeneracy in the spin subspace of the exciton states.

In the following, we derive the EOM for $p_{k\sigma}=\langle a^{\dagger}_{ck\sigma}a_{vk\sigma}\rangle$. The total polarization $\langle P\rangle$, which is equal to $\Sigma_{k\sigma}[\mu_{vc}(k)p_{k\sigma}+\mu_{cv}(k)p^{*}_{k\sigma}]$, can be easily obtained by integration over all k's. In general, terms of the form $\Sigma_{k_1k_2k_3}\Sigma_{\sigma'}\mathcal{V}^{k_1k_2k_3k}_{\lambda_1\lambda_2\lambda_3\lambda}a^{\dagger}_{\lambda_1k_1\sigma}a^{\dagger}_{\lambda_2k_2\sigma'}a_{\lambda_3k_3\sigma'}a_{\lambda k\sigma}$ are encountered in the derivation. By using the random-phase approximation (RPA), the mean values of the product of four operators can be factorized,

$$\begin{aligned}\langle a^{\dagger}_{\lambda_1k_1\sigma}a^{\dagger}_{\lambda_2k_2\sigma'}a_{\lambda_3k_3\sigma'}a_{\lambda_4k_4\sigma}\rangle &= \langle a^{\dagger}_{\lambda_1k_1\sigma}a_{\lambda_4k_1\sigma}\rangle\langle a^{\dagger}_{\lambda_2k_2\sigma'}a_{\lambda_3k_2\sigma'}\rangle\delta_{k_1k_4}\delta_{k_2k_3}\\ &\quad-\langle a^{\dagger}_{\lambda_1k_1\sigma}a_{\lambda_3k_1\sigma}\rangle\langle a^{\dagger}_{\lambda_2k_2\sigma}a_{\lambda_4k_2\sigma}\rangle\delta_{k_1k_3}\delta_{k_2k_4}\delta_{\sigma\sigma'}.\end{aligned} \tag{2.5}$$

After a straightforward but tedious calculation, we have

$$\begin{aligned}i\hbar\frac{\partial p_{k\sigma}}{\partial t}&=(\epsilon_{vk}-\epsilon_{ck})p_{k\sigma}+E(t)\mu_{vc}(k)(n_{vk\sigma}-n_{ck\sigma})\\ &\quad-\sum_{k'}\Bigg[(\mathcal{V}^{kk'}_{vvvv}-\mathcal{V}^{kk'}_{cvcv})(n_{vk'\sigma}-n_{ck'\sigma})\\ &\quad-\sum_{\sigma'}(\tilde{\mathcal{V}}^{kk'}_{vvvv}-\tilde{\mathcal{V}}^{kk'}_{cvvc})(n_{vk'\sigma'}-n_{ck'\sigma'})\Bigg]p_{k\sigma}\\ &\quad+\sum_{k'}\Bigg[\mathcal{V}^{kk'}_{vccv}p_{k'\sigma}+\mathcal{V}^{kk'}_{vvcc}p^{*}_{k'\sigma}\\ &\quad-\sum_{\sigma'}(\tilde{\mathcal{V}}^{kk'}_{vcvc}p_{k'\sigma'}+\tilde{\mathcal{V}}^{kk'}_{vvcc}p^{*}_{k'\sigma'})\Bigg](n_{vk\sigma}-n_{ck\sigma})\\ &\quad+\sum_{k'}\Bigg[\mathcal{V}^{kk'}_{vvcv}n_{vk'\sigma}+\mathcal{V}^{kk'}_{vccc}n_{ck'\sigma}\\ &\quad-\sum_{\sigma'}(\tilde{\mathcal{V}}^{kk'}_{vvvc}n_{vk'\sigma'}+\tilde{\mathcal{V}}^{kk'}_{vccc}n_{ck'\sigma'})\Bigg](n_{vk\sigma}\\ &\quad-n_{ck\sigma}),\end{aligned} \tag{2.6}$$

where $n_{c,vk\sigma}=\langle a^{\dagger}_{c,vk\sigma}a_{c,vk\sigma}\rangle$ are the one-electron occupation numbers in the conduction or valence band, $\mathcal{V}^{kk'}_{\lambda_1\lambda_2\lambda_3\lambda}$ and $\tilde{\mathcal{V}}^{kk'}_{\lambda_1\lambda_2\lambda_3\lambda}$ are abbreviations for $\mathcal{V}^{kk'kk'}_{\lambda_1\lambda_2\lambda_3\lambda}$ and $\mathcal{V}^{kk'k'k}_{\lambda_1\lambda_2\lambda_3\lambda}$, respectively. The terms that are quadratic in $p_{k\sigma}$ are neglected in Eq. (2.6), because only the linear response of the probe wave is considered. Also, relations such as $\mathcal{V}^{kk'}_{cccc}=\mathcal{V}^{kk'}_{vvvv}$ and $\mathcal{V}^{kk'}_{cvcv}=\mathcal{V}^{kk'}_{vcvc}$ have been used, which are based on the symmetry between the conduction band and valence band in the present model. Note that the potential matrix elements with unequal numbers of c and v indices result in the last three lines of Eq. (2.6). These matrix elements are multiplied by terms quadratic in electron or hole occupations, which under resonant pumping may be large. Notwithstanding, because of inversion symmetry, it can be shown that for thermalized exciton gas, these terms actually have no effect on the dynamics (see the Appendix). Consequently, Eq. (2.6) becomes

$$\begin{aligned}[(\epsilon_{ck}-\epsilon_{vk})-\omega-i\gamma]\bar{p}_{k\sigma}(\omega)&=E(\omega)\mu_{vc}(n_{vk\sigma}-n_{ck\sigma})\\&-\sum_{k'}\Big[(\mathcal{V}^{kk'}_{vvvv}-\mathcal{V}^{kk'}_{cvcv})(n_{vk'\sigma}-n_{ck'\sigma})\\&-\sum_{\sigma'}(\tilde{\mathcal{V}}^{kk'}_{vvvv}-\tilde{\mathcal{V}}^{kk'}_{cvvc})(n_{vk'\sigma'}-n_{ck'\sigma'})\Big]\bar{p}_{k\sigma}(\omega)\\&+\sum_{k'}\Big[\mathcal{V}^{kk'}_{vccv}\bar{p}_{k'\sigma}(\omega)+\mathcal{V}^{kk'}_{vvcc}\bar{p}^{*}_{k'\sigma}(-\omega)\\&-\sum_{\sigma'}[\tilde{\mathcal{V}}^{kk'}_{vcvc}\bar{p}_{k'\sigma'}(\omega)+\tilde{\mathcal{V}}^{kk'}_{vvcc}\bar{p}^{*}_{k'\sigma'}\\&\times(-\omega)]\Big](n_{vk\sigma}-n_{ck\sigma}),\end{aligned}\tag{2.7}$$

where $\bar{p}_{k\sigma}=(p_{k\sigma}+p_{-k\sigma})/2$, and a damping term $i\gamma$ has been added. Notice that $\bar{p}^{*}_{k\sigma}(-\omega)\neq\bar{p}_{k\sigma}(\omega)$ because $\hat{p}_{k\sigma}$ is not Hermitian. Therefore, Eq. (2.7) has to be solved in conjunction with the equation satisfied by $\bar{p}^{*}_{k\sigma}$, which is similar to Eq. (2.7) but with ω replaced by $-\omega$ and $\bar{p}_{k\sigma}$ replaced by $\bar{p}^{*}_{k\sigma}$. The meaning of the various parts on the right-hand side of the equation is explained below: The first square bracket, after being summed over k', contributes to the band-gap renormalization. The magnitude of renormalization depends on the strength of interelectron interaction, *as well as* the electron populations. Inside the second square bracket, the $\mathcal{V}^{kk'}_{vccv}$ term is most crucial to the formation of excitons; the $\mathcal{V}^{kk'}_{vvcc}$ term is related to the singlet-triplet splitting of the exciton levels and leads to an unusual coupling between positive and negative frequency components of the polarization. It will be shown in the next section that $\tilde{\mathcal{V}}^{kk'}_{vvvv}=\tilde{\mathcal{V}}^{kk'}_{cvvc}$ because of the charge neutrality condition. We can also show that $\tilde{\mathcal{V}}^{kk'}_{vcvc}$ and $\tilde{\mathcal{V}}^{kk'}_{vvcc}$ are simply constants and can be treated as corrections to $\mathcal{V}^{kk'}_{vccv}$ and $\mathcal{V}^{kk'}_{vvcc}$. The only unknowns in Eq. (2.7) are $\{\bar{p}_{k\sigma}(\omega),\bar{p}^{*}_{k\sigma}(-\omega)\}$. All of the other quantities, including the potential matrix elements and the electron populations, can be obtained given physical conditions such as the strength of electron interaction, the intensity of pump wave, etc. This is derived in the next section.

III. POTENTIAL MATRIX ELEMENT AND ELECTRON POPULATION

A. Potential matrix element

A natural choice for the interaction potential between electrons is $V_0/|\mathbf{r}-\mathbf{r}'|$, where V_0 is given by $e^2/\epsilon a_0$, ϵ is the intrachain dielectric constant, and a_0 is the average distance between neighboring sites. The position r, being dimensionless now, is measured in units of a_0. To calculate $\mathcal{V}^{kk'}_{\lambda_1\lambda_2\lambda_3\lambda_4}$, the unperturbed eigenstates are expanded by localized Wannier functions,[15]

$$\Psi_{\lambda k}(\mathbf{r})=\sum_{j=1,2}u_{\lambda j}(k)\left(\frac{1}{\sqrt{M}}\sum_{m=1}^{M}e^{2ikm}W_{2(m-1)+j}(\mathbf{r})\right),\tag{3.1}$$

where M is the number of unit cells. The total chain length is $2M$. Defining $\zeta_k=[e^{ik}(t_0\cos k-i\delta t\sin k)/\epsilon_{ck}]^{1/2}$, where $t_0-(-1)^l\delta t$ is the hopping amplitude between neighboring sites, then

$$\begin{pmatrix}u_{c1}(k) & u_{c2}(k)\\ u_{v1}(k) & u_{v2}(k)\end{pmatrix}=\begin{pmatrix}\zeta^{*}_k & \zeta_k\\ -\zeta^{*}_k & \zeta_k\end{pmatrix}.\tag{3.2}$$

When calculating the matrix elements of $V_{ee}(\mathbf{r}-\mathbf{r}')$, only the integrals involving Wannier functions at the same site are kept (zero differential overlap approximation).[16] To improve upon this, we need to know the shape of atomic orbitals, which will not be considered here. For the same site, there is a finite on-site energy

$$U_0=1/2\int d^3\mathbf{r}d^3\mathbf{r}'\,W^{*}(\mathbf{r})W^{*}(\mathbf{r}')V_{ee}(\mathbf{r}-\mathbf{r}')W(\mathbf{r}')W(\mathbf{r}).$$

Since the exact form of the Wannier function is not known, U_0 is treated as a parameter independent of V_0. So our choice of the potential is essentially of the Pariser-Parr-Pople form. Defining

$$V_1(q)=\frac{1}{M}\sum_m V_{ee}(2m+1)e^{-i(2m+1)q},$$

$$V_2(q)=\frac{1}{M}\sum_m V_{ee}(2m)e^{-2imq},\tag{3.3}$$

then a straightforward calculation gives

$$\begin{aligned}\mathcal{V}^{kk'}_{\lambda_1\lambda_2\lambda_3\lambda_4}&=V_2(q)\left[\sum_{j=1}^{2}u^{*}_{\lambda_1 j}(k)u^{*}_{\lambda_2 j}(k')u_{\lambda_3 j}(k)u_{\lambda_4 j}(k')\right]\\&+V_1(q)[e^{iq}u^{*}_{\lambda_1 2}(k)u^{*}_{\lambda_2 1}(k')u_{\lambda_3 1}(k)u_{\lambda_4 2}(k')\\&+e^{-iq}u^{*}_{\lambda_1 1}(k)u^{*}_{\lambda_2 2}(k')u_{\lambda_3 2}(k)u_{\lambda_4 1}(k')],\end{aligned}$$

$$\widetilde{\mathcal{V}}^{kk'}_{\lambda_1\lambda_2\lambda_3\lambda_4}=\frac{1}{2}\,V_2(0)+V_1(0)\times[u^*_{\lambda_1 2}(k)u^*_{\lambda_2 1}(k')u_{\lambda_3 1}(k')u_{\lambda_4 2}(k)+u^*_{\lambda_1 1}(k)u^*_{\lambda_2 2}(k')u_{\lambda_3 2}(k')u_{\lambda_4 1}(k)], \tag{3.4}$$

where $q=k-k'$. We require $V_1(0)+V_2(0)=0$ because of the charge neutrality condition. After combining Eq. (3.4) with Eq. (3.2), it can be shown that $\widetilde{\mathcal{V}}^{kk'}_{vvvv}-\widetilde{\mathcal{V}}^{kk'}_{cvvc}=[V_2(0)+V_1(0)]/2=0$, and $\widetilde{\mathcal{V}}^{kk'}_{vcvc}=\widetilde{\mathcal{V}}^{kk'}_{vvcc}=[V_2(0)-V_1(0)]/2$. We emphasize that this nonzero correction is crucial to the reduction of the exciton binding energy when U_0 is tuned to a larger value while keeping V_0 fixed. The same behavior is observed by Abe, Yu, and Su,[15] where their concern is the energy spectrum of the excitons.[17]

B. Electron population

The electron population can be linked to the exciton population by using the method developed by Haug, Koch, and Schmitt-Rink. Their relation is derived below. First, the connection between electron operators and an exciton creation operator $e^\dagger_{njmK}$ is[10]

$$a^\dagger_{ck_1\sigma_1}a_{vk_2\sigma_2}=\frac{1}{\sqrt{2M}}\sum_{njm}\langle jm|\sigma_1\sigma_2\rangle\,\phi^*_{njm}(k)e^\dagger_{njmK}, \tag{3.5}$$

where $\langle jm|\sigma_1\sigma_2\rangle$ is the Clebsh-Gordon coefficient, $k=(k_1+k_2)/2$, $K=k_1-k_2$, and $\phi_{njm}(k)$ is the wave function of an exciton at the nth bound state with angular momentum $\{jm\}$. Helped by this relation, we can write $n_{c,vk}$ in terms of exciton operators as follows: By using an identity operator

$$I=\frac{1}{N_c}\left(N-\sum_{k\sigma}a^\dagger_{vk\sigma}a_{vk\sigma}\right)=\frac{1}{N_c}\sum_{k\sigma}a_{vk\sigma}a^\dagger_{vk\sigma}, \tag{3.6}$$

where N is the total number of electrons and N_c is the number of conduction electrons, we have

$$\hat{n}_{ck_1}\equiv\sum_{\sigma_1}\hat{n}_{ck_1\sigma_1}=\frac{1}{N_c}\sum_{k_2\sigma_1\sigma_2}a^\dagger_{ck_1\sigma_1}a_{ck_1\sigma_1}a_{vk_2\sigma_2}a^\dagger_{vk_2\sigma_2}=\frac{1}{2MN_c}\sum_{nn'jm}\sum_{k_2}\phi^*_{njm}(k)\phi_{n'jm}(k)e^\dagger_{njmK}e_{n'jmK}. \tag{3.7}$$

For a dilute exciton gas, the exciton number $\langle e^\dagger_{njmK}e_{n'jmK}\rangle\simeq g_{njmK}\delta_{nn'}$, where g_{njmK} is the thermal distribution of excitons.[10] Therefore,

$$n_{ck_1}=\frac{1}{2MN_c}\sum_{nk_2}[|\phi^s_n(k)|^2g^s_{nK}+3|\phi^t_n(k)|^2g^t_{nK}], \tag{3.8}$$

where the subscripts s and t stand for ''singlet'' ($j=0$, $m=0$) and ''triplet'' ($j=1$, $m=\pm1,0$) respectively; the factor 3 in front of g^t_{nK} accounts for the triplet degeneracy. For a one-dimensional system, the exciton wave function near band bottom can be approximated by[7] $\phi^{s,t}_0(k)=(2r^{s,t}_0/\pi)^{1/2}/\{1+[(k\pm\pi/2)r^{s,t}_0]^2\}$, where $r^{s,t}_0$ are the radii of the excitons. Note that the conduction band bottoms are at $\mp\pi/2$. The ground state makes a major contribution since all the other levels are far off resonance and barely occupied. According to the single configuration interaction (SCI) calculation of Abe, Yu, and Su,[15] the ratio U_0/V_0 determines whether the singlet exciton level (^1B_u) or the triplet exciton level (^3B_u) is lower in energy. They found that, for $V_0=t_0$ and $U_0>1.39V_0$, ^3B_u is lower than ^1B_u, and vice versa. All the even-parity A_g states are lying at higher energies. However, it is found in some finite-chain calculations that the lowest excitation is actually an even-parity state.[18] This would have a significant effect on the efficiency of luminescence since the optically excited electrons at ^1B_u may relax to the A_g state first, then release their energy via nonradiative channels. Nonetheless, it has been shown that the relaxation rate from the $1\,^1B_u$ exciton to the $2\,^1A_g$ exciton is much smaller than the relaxation rate to the ground state.[19] Furthermore, from the point of view of phase space filling, both $1\,^1B_u$ and $2\,^1A_g$ excitons contribute almost equally to the reduction of phase space. Both factors seem to diminish the effect of this even-parity state. In fact, for the optical nonlinearity being studied, one study shows that, for both SCI and finite-chain calculations, the optical nonlinearity is determined almost entirely by the odd-parity ^1B_u exciton, a dominant A_g exciton above the ^1B_u level (not considered here), and the threshold of the conduction band.[20] Therefore, as far as optical nonlinearity is concerned, we will neglect the influence of this even-parity state in this paper.

The thermal distribution of excitons is given by $g^{s,t}_{nK}=(\exp\{\beta[\epsilon^{s,t}_n(K)-\mu_{s,t}]\}-1)^{-1}$, where $\epsilon^{s,t}_n(K)=\epsilon^{s,t}_n(0)+\hbar^2K^2/2m_{\rm ex}$ are the energies of excitons, the exciton effective mass $m_{\rm ex}$ is $\hbar^2/a_0^2t_0$, and $\mu_{s,t}$ are the quasichemical potentials. Immediately after the optical pumping, there are only singlet excitons because of the selection rule. Part of these excitons then fall down to the triplet level via spin-orbital interaction. Their populations are controlled by the quasichemical potentials in our calculation.

After summing over all the electrons in the conduction band, we have

$$N_c=\sum_{k_1}\hat{n}_{ck_1}=\frac{1}{2MN_c}\sum_{nn'jm}\sum_{kK}\phi^*_{njm}(k)\phi_{n'jm}(k)e^\dagger_{njmK}e_{n'jmK}=\frac{1}{N_c}\sum_{njmK}e^\dagger_{njmK}e_{njmK}, \tag{3.9}$$

where we have used the completeness relation for the exciton wave functions. By taking the expectation value of Eq. (3.9), we have

$$\sum_{njmK}\langle e^\dagger_{njmK}e_{njmK}\rangle=N_c^2. \tag{3.10}$$

This identity is used to determine the values of the chemical potentials μ_s and μ_t, once the total population of, and the relative populations between singlet and triplet excitons are given.

IV. ABSORPTION SPECTRA: NUMERICAL RESULT

Most of this section is devoted to the calculation of the resonant nonlinear optical spectra of PDA for reasons stated in the Introduction. At the end of this section we will comment briefly on the calculation for polyphenylene vinylene (PPV).

PDA has four carbon atoms per unit cell, and consequently four bands in the tight-binding approximation. Since our focus is on the exciton state within the band gap, which is composed of the electron and hole from the middle two bands (conduction and valence band), the outer two bands can be safely neglected. We choose the dimerization-induced band gap, $4\delta t$, to be the unit of energy. The value of t_0, which determines the total band width of conduction band and valence band, is chosen to be 1.25.[21] The average bond length of PDA is 1.35 Å.[15] The Coulomb interaction parameter $V_0 = e^2/\epsilon a_0$ can be determined from the intrachain dielectric constant ϵ. According to the Kramers-Kronig analysis of the reflectivity and with permittivity measurements, this value is close to 3.[22] We choose $\epsilon = 3.5$, such that $V_0 = 2.84$ eV, to fit the calculated exciton binding energy with the value observed in experiments. In most of the following calculations the on-site energy $U_0 = 2V_0$.[15] We have also done several calculations using different choices of U_0 and V_0 values (see Fig. 4). In all of the following calculations the number of sites is 400 and the damping γ is 0.02. We have done calculations on a larger system with 800 sites and confirmed that the finite-size effect is unimportant.

Figure 1 displays the electric susceptibility $\chi(\omega)$, in room temperature, for various concentrations of the singlet exciton gas. The percentages of electrons excited from the valence band by the pump wave are indicated in the legend. The absorption peak in $\mathrm{Im}\chi(\omega)$ can be clearly identified at $\hbar\omega = 1.39$ in the absence of pumping (the solid line). The renormalized band gap is determined by the first maximum of $\mathrm{Im}\chi(\omega)$ beyond the exciton peak, which is barely observable at $\hbar\omega = 1.71$. Notice that the band-gap renormalization due to the Coulomb interaction is quite large. With different exciton populations, the magnitude of renormalization also changes [see the discussion after Eq. (2.7)]. The exact value of the conduction-band edge is difficult to measure experimentally because most of the oscillator strength is ''concentrated'' on the exciton peak. On the other hand, the singlet exciton absorption peak at 1.97 eV is one of the few values that can be determined accurately and is generally agreed upon by researchers.[9,13,19] Therefore, it is used to set the overall energy scale and that means $1.39 \times 4\delta t = 1.97$ eV, or $4\delta t = 1.42$ eV. Consequently, the position of conduction-band edge is at 2.43 eV in our calculation and the binding energy of the singlet exciton is approximately 0.46 eV. This falls within the range 0.4–0.5 for the values reported.[9,13]

In Fig. 1, the absorption signal is reduced as exciton concentration increases. The reduction is approximately proportional to the number of excited electrons. This is consistent with the picture of PSF, which gives[9]

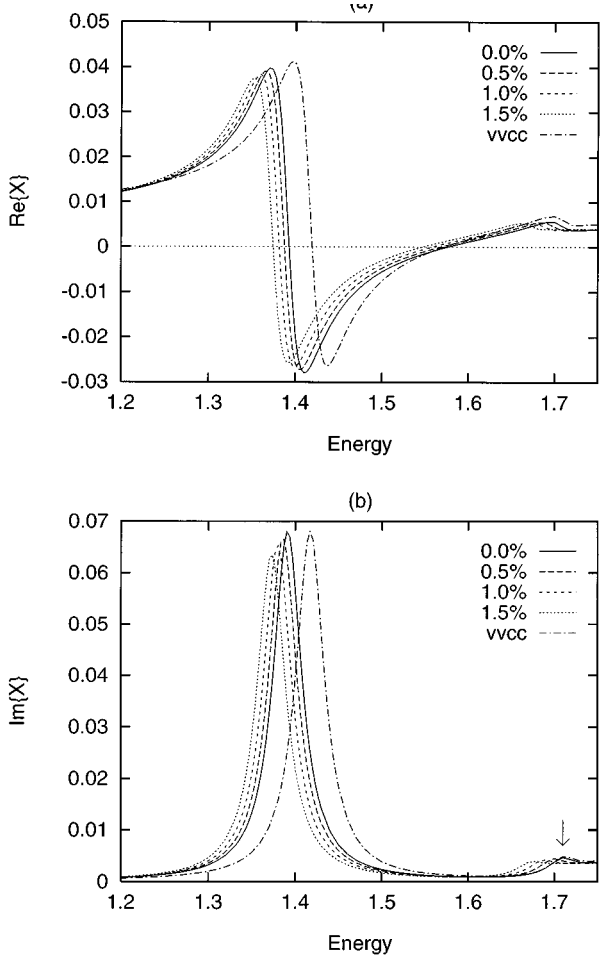

FIG. 1. Real (a) and imaginary (b) parts of $\chi(\omega)$ for different exciton concentrations, labeled by the percentages of the occupation of conduction band (0, 0.5%, 1.0%, and 1.5%) at room temperature. Probe energy is in units of the bare band gap, $4\delta t$. The ''$vvcc$'' curve comes from the calculation without the $\mathcal{V}^{kk'}_{vvcc}$ and $\tilde{\mathcal{V}}^{kk'}_{vvcc}$ terms and in the absence of excitons. The arrow at the bottom right of Fig. 1(b) indicates the position of the band edge for the solid line.

$$\delta f/f = -n_{\mathrm{ex}}/n_{\mathrm{ex}}^{\mathrm{sat}}, \tag{4.1}$$

where f is the oscillator strength, n_{ex} is the exciton density per unit length, and $n_{\mathrm{ex}}^{\mathrm{sat}}$ is the saturation density, at which exciton wave functions begin to overlap in space. By using Eq. (4.1), we can estimate the exciton radius and the result is about five unit cells, which is again consistent with earlier calculations.[13,15]

Figure 2 shows the absorption coefficient α and the change of refraction index δn near the exciton peak. The values of the exciton concentration are the same as in Fig. 1. The chain-to-chain distance for PDA in the crystalline phase is about 10 Å,[9] and the intersite distance is 1.4 Å. Therefore, 1% concentration has 7.1×10^{19} cm^{-3} conduction electrons. The pump intensities I_p required for this electron concentration n_{ex} can be obtained from $I_p = n_{\mathrm{ex}}\hbar\omega_p/\alpha_t\tau$ (reflection from the sample is ignored), where $\hbar\omega_p = 1.97$ eV, the peak absorption α_t (including π electrons and the background) is approximately 10^6 cm^{-1},[7] and the recombination time τ is 2 ps.[9] Consequently, to excite 7.1×10^{19} cm^{-3} electrons requires a pump wave with intensity $I_p = 1.14 \times 10^7$ W/cm^2. The optical Kerr coefficient n_2, which measures the change

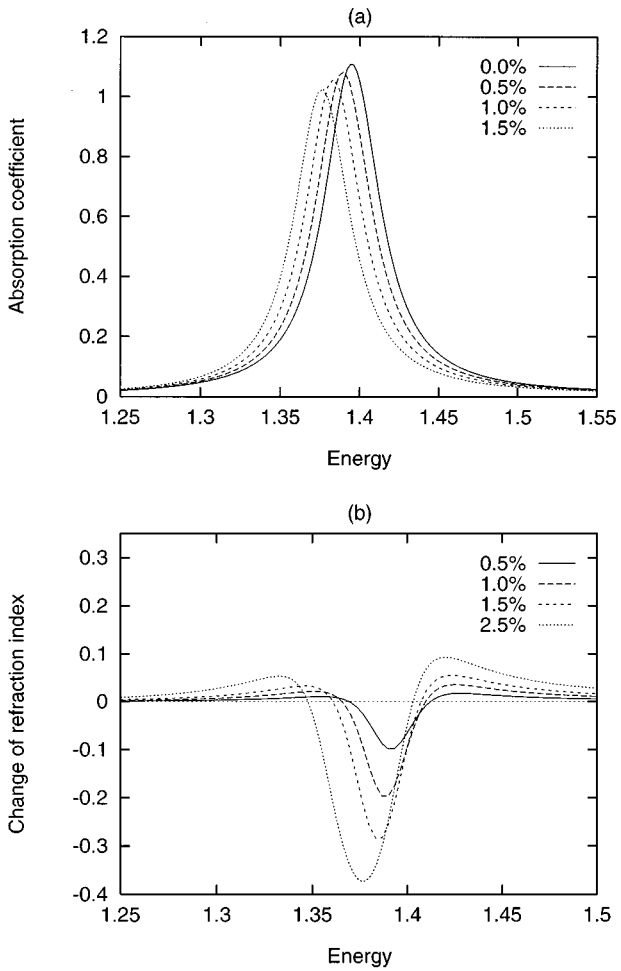

FIG. 2. The effect of different exciton concentrations on (a) absorption coefficient α and (b) the change of refraction index δn. α is in units of 2.0×10^4 cm^{-1}. The energy is in units of $4\delta t$.

of refraction index due to pumping, is given by $n_2=|\delta n|/\delta I_p$. For a pulse with $I_p=1.14\times10^7$ W/cm^2, we have $|\delta n|=0.196$ at resonance [see Fig. 2(b)] and, therefore, $n_2=1.7\times10^{-8}$ cm^2/W. This is four orders of magnitude larger than the nonresonant value, and is close to the observation of Greene *et al.*, 3.0×10^{-8} cm^2/W.[9]

All of the above calculations are for singlet excitons at room temperature. Using the same formalism it is quite easy to investigate the influence of exciton species and temperature on the resonant nonlinearity. We consider a two-level model where only the singlet (^1B_u) and triplet (^3B_u) excitons are considered. The exciton radii are chosen to be $6a$ (r_0^s) and $4.5a$ (r_0^t).[15] In Fig. 3, we show the extreme cases where the populations are either all singlet or all triplet. This difference traces back to the different distributions of the relative part of the electron-hole pair wave functions $\phi_0^{s,t}(k)$. It can be seen that the difference between singlet and triplet curves is more significant at low temperature (10 K). Such a temperature effect has not been studied experimentally, however.

In Fig. 4, we show how different choices of the strength of the electron-electron interaction may affect the absorption spectra. It can be seen that the magnitude of V_0, the long-range interaction, has significant effect on the band-gap renormalization and the binding energy. For example, the

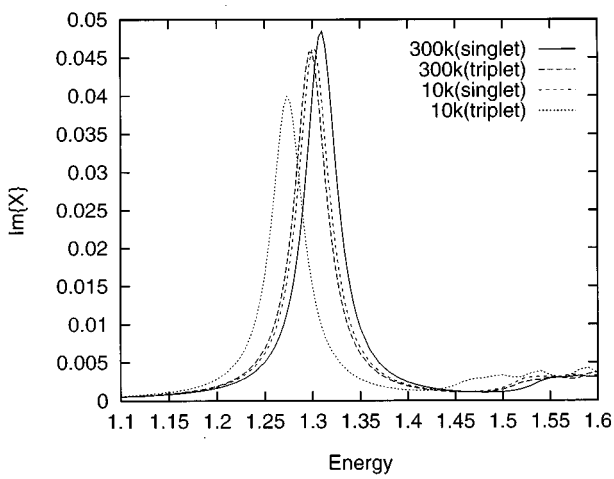

FIG. 3. The effect of temperatures and singlet/triplet populations on Im$\chi(\omega)$. The percentage of conduction electrons is 2.5% for all of the curves. At room temperature, it makes small difference whether the excitons are singlet or triplet. The distinction is more apparent at 10 K.

band edges for $U_0=4$ and $V_0=1.5$, 2, 2.5 are at 1.54, 1.71, and 1.89, respectively (see arrows in the figure). The widths of the band gap vary roughly linearly with V_0. On the other hand, the short-ranged on-site energy U_0 has little influence on the band gap. Furthermore, contrary to the effect of V_0, a larger U_0 leads to a smaller binding energy. This adverse effect can be traced back to the exchange terms $\tilde{\mathcal{V}}^{kk'}_{\lambda_1\lambda_2\lambda_3\lambda_4}$ in Eq. (3.4). The dependence of the position of the exciton level on U_0 and V_0 resembles closely the calculations by Abe, Yu, and Su.[15]
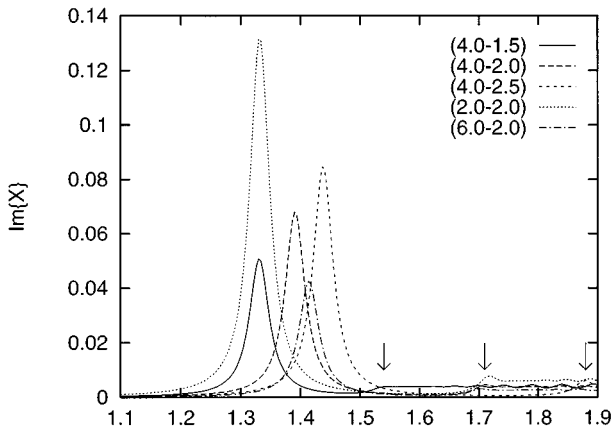
This work is based on the simplified model of an infinite and rigid chain and seems to be applicable to other conjugated polymers with exciton levels as well, such as PPV and polysilane.[23,24] At the end of this section, we present a cal-